[CANCER RESEARCH 60, 7084–7093, December 15, 2000]

A Role for the Integrin αvβ8 in the Negative Regulation of Epithelial Cell Growth[1]

Stephanie Cambier, De-zhi Mu, David O'Connell, Kevin Boylen, William Travis, Wei-hong Liu, V. Courtney Broaddus, and Stephen L. Nishimura[2]

Departments of Anatomic Pathology [S. C., D-z. M., D. O., K. B., S. L. N.], Medicine [W-h. L., V. C. B.], and the Lung Biology Center [S. C., D-z. M., D. O., K. B., W-h. L., V. C. B., S. L. N.], University of California at San Francisco, San Francisco, California 94143, and the Pulmonary and Mediastinal Pathology Section of the Armed Forces Institute of Pathology, Washington, DC 20306 [W. T.]

ABSTRACT

The control of cell growth is regulated through coordinated responses to growth factors and cell-extracellular matrix (ECM) interactions. Integrins, the major family of cell-ECM receptors, are vital to these coordinated responses. Although much is known of the role of integrins in growth promotion, specific examples of integrin-mediated cell growth inhibition are few. On the basis of our findings that the integrin β8 subunit is expressed in airway epithelial cells and is absent in lung cancers, we investigated the role and mechanism of the integrin αvβ8 in mediating growth inhibition. When introduced into either a lung or colon carcinoma cell line, β8 inhibited cell growth without inducing apoptosis. Ligation of αvβ8 also induced cell rounding, inhibited focal contact formation, and initiated an inhibitory signaling pathway as demonstrated by increased expression of the cyclin-dependent kinase inhibitor $p21^{Cip1}$. The cytoplasmic domain of β8 was capable of both growth inhibition and causing cell shape changes as shown by the use of a chimeric integrin construct consisting of the β8-cytoplasmic domain coupled to the β6-extracellular domain. Finally, when tested *in vivo*, β8 potently inhibited tumor growth in nude mice. Together, these results implicate αvβ8 as a novel growth-regulatory molecule of epithelial cells.

INTRODUCTION

Integrins, the major family of cell adhesion receptors that mediate cell-ECM[3] interactions, appear to play a major role in the regulation of cell proliferation. Considerable attention has focused on the αv subfamily of integrins because αvβ3, αvβ5, and αvβ6 have been shown to promote tumor growth, metastasis, and angiogenesis (1–5). However, these growth-promoting αv integrins are present on many cell types with a slow rate of growth such as airway epithelium (6–10), suggesting that these cells possess mechanisms that oppose growth-promoting integrin signals. Understanding the control of balanced growth in airway epithelium is of particular importance because of the role that dysregulated proliferation of airway epithelium plays in the pathogenesis of lung cancer, the leading cause of cancer mortality worldwide (11, 12).

The β1, β3, β5, and β6 integrin subunits may initiate growth-promoting signaling cascades through their highly homologous integrin β subunit cytoplasmic domains. Mutational analysis has identified conserved motifs in these highly homologous cytoplasmic domains required for adhesive functions, localization to focal contacts, and interactions with signaling molecules such as FAK (1, 13–18). Evidence is emerging, however, that these growth-promoting integrin signals may be counterbalanced via inhibitory integrin signaling pathways (19–22). These inhibitory pathways can be engaged through unique integrin β cytoplasmic domains produced either through alternative splicing or evolutionary divergence (22).

The integrin αvβ8, a VN receptor, is of particular interest as a potential negative regulator of cell growth for several reasons: (*a*) the cytoplasmic domain of β8 is divergent in sequence, lacking all amino acid homology with the highly homologous cytoplasmic domains of the other αv-associating integrin β subunits (β1, β3, β5, and β6; Refs. 13 and 23); (*b*) the β8 cytoplasmic domain is divergent in function because the cytoplasmic domain of β8 cannot support stable cell adhesion to VN, although soluble αvβ8 can bind avidly to VN using affinity chromatography (24). In fact, when the β8 cytoplasmic domain is combined with the β3 extracellular domain in a chimeric receptor, β3-mediated adhesion to VN is abolished (24); and (*c*) αvβ8 has a restricted distribution and is most highly expressed in nonproliferating cell types (25).

In this study, we found that the αvβ8 integrin is expressed in airway epithelial cells *in vivo* and *in vitro* and is generally absent in lung cancer. To test whether the divergent β8 subunit is growth inhibitory, we reconstituted β8 in lung and colon cancer cells. We now report that β8 inhibits cell growth both *in vitro* and *in vivo* and, using a chimeric mutant, have implicated the β8 cytoplasmic domain in this function. These results identify β8 as a potential novel growth-regulatory molecule of the human airway.

MATERIALS AND METHODS

Cell Lines and Reagents. The lung cancer cell lines UCLA P3 and A549 and the colon carcinoma cell line SW480 were obtained from the American Type Culture Collection (Bethesda, MD). The lung cancer cell lines NCI H23, H226, H358, H596, H647, H676, H727, H838, H996, H1264, H1299, H1650, H1710, H1734, and H1792 are cell lines from the National Cancer Institute lung cancer cell line collection and categorized based on histology of the parental tumor and mutational spectrum (26–28) and were a generous gift of Dr. Herbert Oie (National Cancer Institute, Bethesda, MD). The transformed airway epithelial cell lines 16NBE14o- and 1HAEo- were a gift of Dr. Dieter Gruenert (UCSF, San Francisco, CA; Refs. 29 and 30). NHBE cells were obtained from commercial sources (Clonetics, San Diego, CA). The amphotrophic retroviral packaging line Phoenix was a gift of Dr. Garry Nolan (Stanford University, Palo Alto, CA; Ref. 31). The following antibodies were used: mouse anti-β8 (SN1; Ref. 24), anti-β3 (American Type Culture Collection; Ref. 32), anti-β6 (E7P6; Ref. 33), anti-β5 (P1F6; Chemicon; Ref. 33), anti-αv (L230; Ref. 33), polyclonal rabbit anti-β5 (gift of Dr. Louis Reichardt, UCSF, San Francisco, CA), affinity-purified rabbit anti-β8 (25), affinity-purified rabbit anti-glutathione *S*-transferase (25), mouse antihuman vinculin (Sigma Chemical Co., St. Louis, MO), mouse anti-BrdUrd (Dako, Copenhagen, Denmark), rabbit anti-FAK (Santa Cruz Biotechnology, Santa Cruz, CA), rhodamine-phalloidin (Sigma), rabbit-anti p21 (C-19; Santa Cruz Biotechnology), and rat antihuman heat shock protein 90 α subunit (9D2; StressGen Biotechnologies, Victoria, British Columbia, Canada). The secondary antibodies and conjugates used were: phycoerythrin-goat antimouse, rhodamine-donkey antirabbit (Chemicon, Temecula, CA), phycoerythrin-goat antimouse, rhodamine-goat antimouse (The Jackson Immunoresearch Laboratory, Inc., Westgrove, PA), HRP conjugated sheep antimouse (Amersham), HRP-antirat

Received 6/20/00; accepted 10/31/00.

The costs of publication of this article were defrayed in part by the payment of page charges. This article must therefore be hereby marked *advertisement* in accordance with 18 U.S.C. Section 1734 solely to indicate this fact.

[1] This work was supported by Grants KO8 CA63143 (to S. L. N.) and RO1 HL8985 (to V. C. B.) from the NIH; grants from the American Cancer Society, American Lung Association, and American Heart Grant-in-Aid (to S. L. N.); and Grant TRT-0051 from the Tobacco-Related Disease Research Program (to V. C. B.).

[2] To whom requests for reprints should be addressed, at Lung Biology Center, Box 0854, University of California at San Francisco, San Francisco, CA 94143. Phone: (415) 206-5906; Fax: (415) 206-4123; E-mail: cdog@itsa.ucsf.edu.

[3] The abbreviations used are: ECM, extracellular matrix; FAK, focal adhesion kinase; VN, vitronectin; BrdUrd, bromodeoxyuridine; Col I, collagen type I; CM, complete media; FACS, fluorescence-activated cell sorter; FN, fibronectin; NHBE, normal human bronchial epithelial cell; HRP, horseradish peroxidase; UCSF, University of California at San Francisco.

(Cappel), HRP-protein A (Amersham), biotinylated sheep antimouse and fluorescein-streptavidin (Amersham, Buckinghamshire, United Kingdom).

Retroviral Vectors and Constructs. Retroviral vectors used were pLXSN (Clontech, San Diego, CA), pBabePuro (gift of Dr. Hartmund Land; Ref. 34) and LZRS (gift of Dr. Garry Nolan, Stanford University, Palo Alto, CA, Imperial Cancer Research Fund, London, UK; Ref. 31). The retroviral vectors pBabeβ8Puro and pLXSNβ8Neo were prepared by subcloning the full-length β8 coding sequence from the β8 expression vector (pcDNA1neoβ8; Ref. 24) into the multiple cloning sites of pBabePuro or pLXSN (Clontech). The β6/8 chimera was constructed in pcDNA1neoβ6 (33) using splice overlap extension PCR (35), using internal primers generated to join the β6 transmembrane and β8 cytoplasmic domains at amino acid 710 of the β8 coding region. The β6 (33) and β6/8 constructs were then transferred into pBabePuro. Plasmids were purified using the Qiagen (Valencia, CA) plasmid purification system. All constructs were sequenced completely through the amplified regions and verified with the exception of a single nucleotide difference found in the β6 transmembrane region that did not agree with the published sequence (36). The resultant amino acid change (position 719 of β6, T to I) most likely represents a sequencing error in the published sequence because the translation of our sequence was in agreement with the mouse β6 sequence (GeneBank accession no. AF115376). Furthermore, this resultant amino acid change (T to I) agreed with the conservation of this amino acid in the transmembrane domain of other integrin β subunits (37). The following antibiotics were used: puromycin, chloroquine (Sigma), geneticin (G418; Life Technologies, Inc., Grand Island, NY), hygromycin (Calbiochem), and Fungizone, penicillin, and streptomycin (UCSF cell culture facility, UCSF). Restriction enzymes and Vent polymerase were from New England Biolabs.

Cell Culture. The Phoenix packaging line, the lung carcinoma cell lines, and the SW480 cell line were maintained in CM consisting of DMEM or RPMI 1640 (Life Technologies, Inc.) supplemented with 10% FCS (Hyclone, Fisher) and penicillin and streptomycin. NHBE cells were maintained in bronchial epithelial growth media supplemented with growth factors and retinoic acid (Clonetics). All cells were maintained at 37°C with 5% CO_2 in humidified water-jacketed CO_2 incubators.

Retroviral Transduction. The Phoenix packaging line was transfected using standard calcium phosphate protocols (31). The lung carcinoma cells were transduced with filtered infectious supernatants, and 48 h after infection, expressing cells were selected in CM with puromycin (4 μg/ml) or G418 (1 mg/ml). Pools of β8-expressing cells were either used within 72 h for short-term experiments or were sorted for uniform expression of β8 and propagated on Col I-coated plates for long-term experiments.

Selection of the Adenosquamous H647 and SW480 Cell Line. We chose several cell lines that did not express αvβ8 as determined by FACS and which showed >30% transduction using the retroviral LAC Z (LZRS) reporter construct (31). Of these, we were able to obtain detectable β8 expression by FACS in several lung cancer cell lines (H647, H727, and H1734) and the colon carcinoma SW480 cell line. When transduced, all four cell lines grew poorly compared with their mock-infected counterparts. We chose the H647 adenosquamous lung carcinoma cell line because it was easy to maintain in cell culture and spread well so that cell morphology could be studied (the parental H1734 and H727 cells were difficult to propagate and spread poorly). We chose the SW480 cell line because it has been characterized extensively, has been shown to proliferate in an integrin-dependent fashion, and has a simplified αv-integrin repertoire (expressing only αvβ5; Refs. 1 and 38).

Fluorescence-activated Cell Analysis and Sorting. For FACS, cells were detached using 7 mM EDTA in DMEM, incubated with primary antibodies for 30 min at 4°C, and detected with phycoerythrin-conjugated secondary antibodies (Chemicon). Stained cells were analyzed using a FACsort flow cytometer and CellQuest software (Becton Dickinson). Pools of β8, β6, and β6/8 and mock-infected cells were stained and sorted (Becton Dickinson FACSvantage) at the same time after retroviral transduction. Composites of histograms were made in Adobe Photoshop 4.01 and QuarkExpress 4.04.

Immunoprecipitation Analysis/Western Blotting. β8-expressing or mock-infected H647 cells in confluent 10-cm dishes were surface-labeled with 0.1 mg/ml NHS-LC-biotin (Pierce Corp., Rockford, IL). Preparation of lysates and αv and β8 immunoprecipitations were as described (24, 25). Immune complexes were resolved by 7.5% SDS-PAGE with prestained markers (Bio-Rad) and transferred to a polyvinylidene difluoride membrane (Millipore), where biotinylated proteins were detected by an HRP-streptavidin conjugate (Amersham) followed by chemiluminescence (ECL; Amersham). For Western blotting, β8-expressing or mock-infected SW480 and H647 cells were plated onto VN or Col I-coated tissue culture dishes and allowed to attach for 24 h in CM prior to harvesting in lysis buffer [10 mM Tris (pH 7.4), 150 mM NaCl, 1% Triton X-100, 0.1% SDS, with protease inhibitors]. Protein quantification was by bicinchoninic acid (Pierce), and 40 μg of proteins were resolved by 12.5% SDS-PAGE. Equal protein loading was always confirmed in parallel, by Ponceau S (Sigma) and/or Coomassie blue (Bio-Rad) staining. As an additional protein loading control, the portion of each blot above the M_r 70,000 prestained marker was separated and analyzed by immunoblotting for heat shock protein 90 (StressGen). Composites of scanned images were assembled in Adobe Photoshop 4.01 and QuarkExpress 4.04. One-dimensional gel analysis was by NIH Image (v1.62).

ECM Proteins, Preparation, and Coating. VN was prepared from outdated fresh frozen human plasma (39). Col I was prepared from rat tails (40). Petri dishes, 24-well dishes (Falcon; Fisher), 96-well plates (Falcon), or glass chamber slides (Structure Probe, Westchester, PA) were coated with VN or Col I for 2 h at 37°C. Coating concentrations ranged from 0.5 to 10 μg/ml. Nonspecific binding sites were blocked using 1% BSA in PBS for 30 min at 37°C.

Immunohistochemistry and Immunocytochemistry. Paraffin-embedded tissue sections were obtained from surgical biopsy specimens from the UCSF and the Armed Forces Institute of Pathology according to institutional guidelines. A total of 37 specimens were evaluated, 30 of which contained neoplastic lung disease and 20 of which contained nonneoplastic airway. Sections underwent standard antigen retrieval (41), followed by immunohistochemical detection of β8 as described (25). Staining of sections was graded by a pulmonary pathologist (S. L. N.) as follows: 0 to 1+, negative to indeterminate epithelial membrane staining; 2+, weak but clearly positive epithelial membrane staining; and 3 to 4+, strong membrane staining. For statistical analysis, negative staining was considered 0–1+, and positive staining was considered 2–4+. For immunocytochemistry, cells were detached and counted, and 5000 cells were allowed to attach (4 h) in CM to individual wells of ECM-coated glass slides. The cells were fixed and permeabilized for 5 min in 2% paraformaldehyde with 0.3% Triton X-100. Primary antibodies were applied followed by biotinylated sheep antimouse (Amersham) or rhodamine-conjugated donkey antirabbit, followed by fluoresceinated-streptavidin conjugate (Amersham) or rhodamine-phalloidin (Sigma). The slides were coverslipped in Vectashield (Vector), sealed, and photographed with a digital imaging system (Kodak) attached to a Nikon epifluorescence inverted phase microscope and assembled into composites in Adobe Photoshop 4.01 and QuarkExpress 4.04.

Cell Adhesion and Spreading Assays. Cell adhesion assays were performed on VN-, FN- or Col I-coated 96-well plates (coating concentration range, 0.5–10 μg/ml) essentially as described (24). Briefly, detached cells (1×10^4 cells in each duplicate of wells) were centrifuged onto the plates at $10 \times g$ for 5 min in DMEM in the presence or absence of antibodies to β5 (P1F6), β6 (10D5), or β1 (P5D2). After incubation for 1 h at 37°C, the plates were inverted and centrifuged for 5 min at $10 \times g$ and then immediately fixed and stained in cell staining buffer (1% formaldehyde, 20% methanol, and 0.5% crystal violet). After dye solubilization in PBS with 0.1% Triton X-100 for 1 h at room temperature, the plates were analyzed on an ELISA plate reader (Bio-Rad) at A_{595}. Background binding was defined as binding of cells adherent to BSA-coated wells. For cell spreading assays, H647 cells (1×10^5) were plated in CM on 10-cm ECM-coated-plates (10 μg/ml coating concentrations), or SW480 cells (1.6×10^5) were plated on coated 24-well dishes (10 μg/ml coating concentrations). For some experiments, β8-expressing H647 or SW480 cells (1.6×10^4) were plated onto 24-well dishes coated with 1, 2.5, 5, 7.5, and 10 μg/ml Col I. After 24 h, at least three random fields (100 cells total) were examined per well in a blinded fashion using a Nikon inverted phase microscope. Experiments were repeated in triplicate. Cells were defined as spread if lamellipodia were present and if the cell borders showed no phase enhancement.

Cell Proliferation and Apoptosis Assays. H647 cells (5×10^5) expressing or not expressing β8 were counted by trypan blue exclusion and plated onto Col I-coated dishes in CM. After 72 h, the cells were detached and used for the following assays. For cell proliferation assays, 2×10^5 β8-expressing and mock-infected H647 cells were plated onto VN- or Col I (0.5–10 μg/ml coating concentration)-coated, 10-cm dishes in CM, grown for 72 h, released by trypsin (0.05%), and counted by trypan blue exclusion. For cell cycle and apoptosis assays, 3×10^5 cells were grown on VN- or Col I-coated dishes for

24 h in CM prior to harvesting by trypsinization (0.25%). The cells were either immediately fixed in 70% ice cold ethanol and used for cell cycle analysis or were stained by double labeling with propidium iodide and annexin V-GFP fusion protein (gift of Dr. Joel Ernst, UCSF, San Francisco, CA) as described for determination of apoptosis (42). For cell cycle analysis, the fixed cells were incubated in RNase (100 μg/ml; Sigma) for 30 min at 37°C, stained in propidium iodide (50 μg/ml; Boehringer-Mannheim), and then analyzed for DNA content by flow cytometry. Statistics on gated quadrants or histograms were generated using CellQuest software (Becton Dickinson). For BrdUrd incorporation assays, the cells were grown on coated glass chamber slides (Structure Probe) in CM. After 16–18 h, 10 μM BrdUrd was added in fresh CM for 5 h before fixation in 3.5% paraformaldehyde for 30 min. The DNA was denatured in 0.2 N HCl for 30 min; the cells were permeabilized in 0.5% NP40 and then incubated in anti-BrdUrd antibody (Dako), followed by rhodamine goat antimouse (Jackson) with Hoechst 33342 (Molecular Probes, Eugene, OR; 2 μg/ml) as a nuclear counterstain. At least 100 labeled nuclei were counted per well and recorded as a percentage of total nuclei, in each experiment, and were repeated multiple times ($n < 3$) using independently transduced pools of cells.

SW480 cells retrovirally transduced with β8, β6, β6/8, or retroviral vector alone were sorted for uniform expression and were used for proliferation assays. Cells from sorted pools (1.6×10^4) were grown in wells of coated 24-well dishes in CM for 72 h, released by trypsin (0.05%), and counted by trypan blue exclusion or stained with annexin V and propidium iodide for determination of apoptosis.

For growth in soft agar, sorted pools of either β8-expressing or mock-infected H647 or SW480 cells (1×10^3) were grown in 0.3% agar (1 ml) in 10% FCS in DMEM in triplicate wells of a 24-well plate. After 2 weeks, colony formation was assessed by counting colonies >100 mm in diameter per five random fields. Assays were counted in a blinded fashion.

Tumorigenicity Assays. Athymic *nu/j* nude mice (The Jackson Laboratory) were s.c. injected with sorted pools of either β8-expressing or mock-infected H647 cells (1×10^6) in each of four sites. After 3 weeks, the mice were sacrificed according to UCSF animal care guidelines. The experiment was repeated three times with three independent sorted pools of β8-expressing and mock-infected H647 cells (six mice/pool/experiment). Tumors from each mouse were counted separately and weighed. Full autopsies were performed to examine organs for metastasis.

Statistical Analysis. Immunohistochemical data were analyzed using contingency tables and Fisher's exact test. For other data, Students' *t* test was used for comparison of two data sets, ANOVA (for parametric data) or the Kruskal-Wallis test (for nonparametric data) were used for more than two data sets. Tukey's or Dunn's test was used for parametric or nonparametric data, respectively, to determine where the differences lay. Significance was defined as $P < 0.05$. Data are shown as means ± 1 SD, unless otherwise noted. Statistical software used was InStat version 2.03 (GraphPad Software, Inc., San Diego, CA).

RESULTS

The β8 Integrin Subunit Is Expressed in Normal Airway Epithelium but not in Pulmonary Neoplasia. The expression of β8 in normal and neoplastic airways was evaluated in 37 pulmonary biopsies representing a broad spectrum of neoplastic and reactive airway diseases including non-small cell carcinoma ($n = 22$), small cell carcinoma ($n = 6$), carcinoid tumors ($n = 2$), inflammatory and/or interstitial lung disease ($n = 5$), and metastatic tumors ($n = 2$). In 100% of the specimens that had benign airway epithelium present for evaluation ($n = 20$), staining for β8 was moderate to intense in the normal epithelium (≥2; Fig. 1*A*). In lung tumor specimens ($n = 30$), although β8 staining was strong in the adjacent normal airway epithelium, the expression of the β8 integrin subunit in the tumors was largely absent (Fig. 1*C*); 97% ($n = 29$) of pulmonary tumors showed negative staining for β8 (≤1+) and only 3% ($n = 1$) showed moderate immunoreactivity for β8 (2+; β8 expression: normal *versus* cancer, $P < 0.0001$).

The Integrin αvβ8 Is Expressed in NHBE Cells and Not in Lung Cancer or Transformed Airway Epithelial Cell Lines. Using FACS, αvβ8 expression was confined to NHBE cells and was essentially undetectable in 17 lung cancer cell lines and 2 transformed airway epithelial cell lines (Fig. 2*A*).

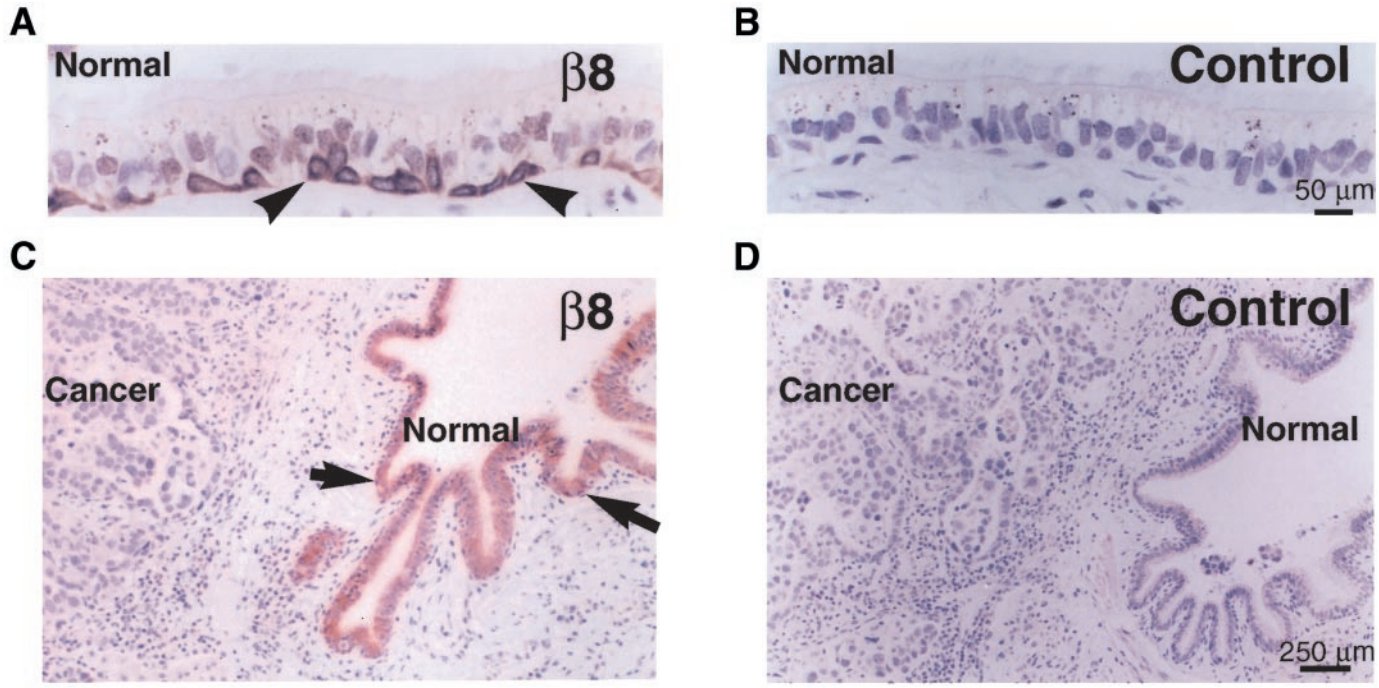

Fig. 1. The β8 subunit is expressed in benign airway epithelium and is absent in lung carcinomas. Paraffin-embedded sections were stained with affinity-purified polyclonal antibodies raised to the β8 cytoplasmic domain (*A* and *C*) or to glutathione *S*-transferase as a control (*B* and *D*; Ref. 25). *A* and *B*, benign airway from a case of nonneoplastic lung disease. *C* and *D*, a case of well-differentiated adenocarcinoma with benign airway adjacent to the carcinoma. Two patterns of airway staining with β8 antibodies are seen. Note that in *A*, there is predominant basal cell labeling (*arrowheads*), and in *C*, there is diffuse staining in all airway epithelial cell types (*Normal*) including the basal cells (*arrows*). No staining is observed in the adenocarcinoma (*Cancer*) or with control antibodies (*B* and *D*).

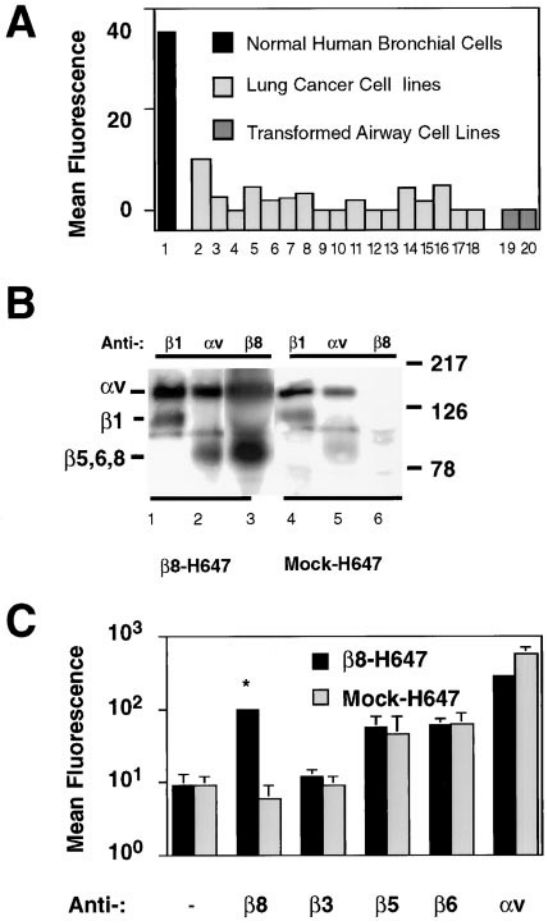

Fig. 2. The integrin αvβ8 is expressed in primary cultures of NHBE cells but is absent from transformed and malignant airway epithelial cell lines. *A*, αvβ8 is expressed in primary cultured NHBE cells but not in 17 lung carcinoma cell lines or two transformed airway epithelial cell lines. Using flow cytometry, β8 expression was assessed using the monoclonal anti-β8 antibody SN1. Data are expressed as the difference in arbitrary mean fluorescence units between cells stained with SN1 and no primary antibody. Shown is a representative experiment. *Columns: 1*, NHBE; *2*, H23; *3*, H226; *4*, H358; *5*, H596; *6*, H 647; *7*, H676; *8*, H727; *9*, H838; *10*, H996; *11*, H1264; *12*, H1299; *13*, H1650; *14*, H1710; *15*, H1734; *16*, H1792; *17*, A547; *18*, UCLA-P3; *19*, 16HBEo-; and *20*, 1HAEo-. *B*, β8 is expressed on the cell surface of β8-transduced H647 cells without changing the surface expression of other αvβ heterodimers. Immunoprecipitation of surface biotinylated cell lysates with anti-β8 revealed two bands migrating (nonreduced) at M_r 150,000 and M_r 90,000 consistent with the electrophoretic migration of the αv and β8 subunits (Ref. 24; *Lane 3*), not seen in mock-infected H647 cells (*Lane 6*). αv (L230) immunoprecipitates (*Lanes 2* and *5*) revealed no evidence of the β1 subunit as shown by β1 immunoprecipitates (*Lanes 1* and *4*). Thus, H647 cells do not express the αvβ1 heterodimer. *Left*, expected migration of the indicated integrin subunits; *right*, migration of prestained molecular weight markers. *Lanes 1–3*, β8-expressing H647 cells; *Lanes 4–6*, mock-infected H647 cells. *C*, when the H647 cells were transduced with β8, the αvβ8 heterodimer was efficiently expressed on the cell surface (*) without significantly affecting the cell surface levels of the other αv integrins present, αvβ5 and αvβ6. Note that no antibody specific for the αvβ1 heterodimer exists. *Bars*, SD.

The Integrin β8 Subunit Can Be Heterologously Expressed as αvβ8 by Retroviral Transduction into Lung Carcinoma Cell Lines. Initially, we had difficulties in obtaining β8 expression using liposome- and calcium phosphate-mediated gene transfer techniques in lung cancer cell lines, possibly because of a toxic or growth-inhibitory effect. Thus, we used a high efficiency retroviral gene transfer method (Ref. 31; 30–50% of all cells were transduced), allowing us to work with pools of expressing cells reflecting the natural heterogeneity of the cell line. Furthermore, these pools could be sorted to achieve uniform β8 expression.

Using immunoprecipitation, we confirmed that the αvβ8 heterodimer was present on the surface of β8-infected H647 cells and not mock-infected cells (Fig. 2*B*). To determine whether β8 expression altered the expression of other αvβ integrins, we measured the levels of other β subunits that pair with αv using flow cytometry or, for αvβ1, immunoprecipitation (Fig. 2, *B* and *C*). Our results demonstrate that the H647 cells normally express αvβ5 and αvβ6 and do not express αvβ1, αvβ3, or αvβ8. Heterologous expression of β8 in H647 cells does not change the endogenous levels of αvβ5 and αvβ6.

Expression of the αvβ8 Integrin Has No Effect on H647 Adenosquamous Lung Cancer Cell Adhesion. αvβ8 expressed by H647 lung carcinoma cells did not mediate cell attachment to VN and did not change the basal levels of adhesion to VN when compared with the mock-infected cells (Fig. 3*A*). Thus, in the presence of

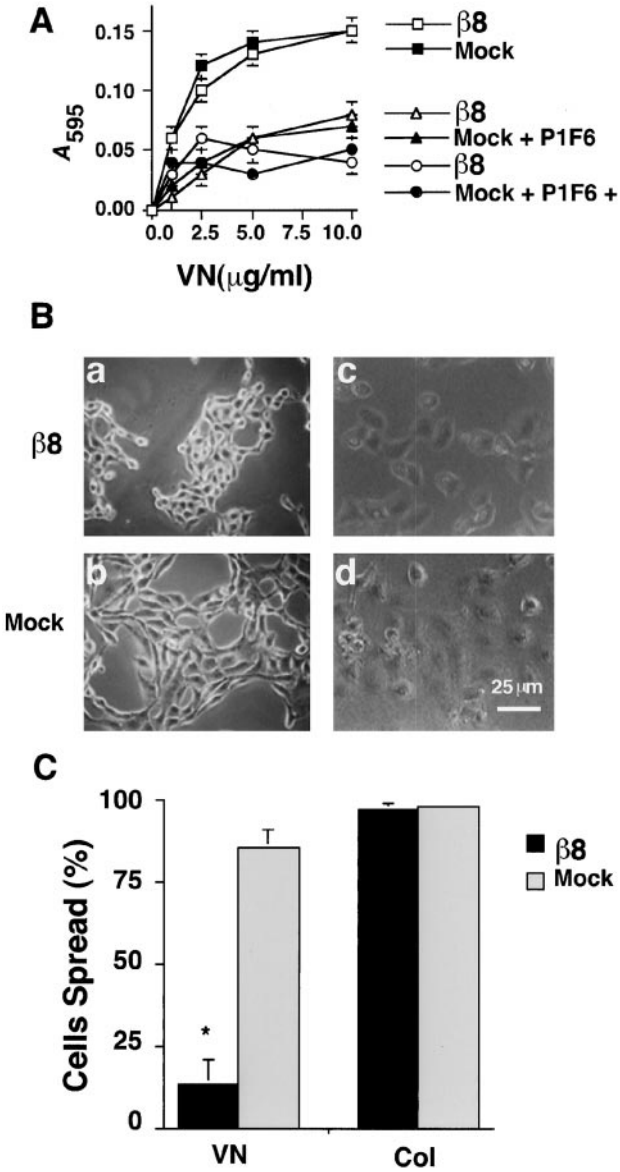

Fig. 3. The integrin αvβ8 does not change the ability of H647 adenosquamous lung carcinoma cells to adhere to VN. *A*, adhesion assays ($n = 12$) to VN were performed using β8-expressing (*β8*) or mock-infected (*Mock*) H647 cells in the presence of anti-β5 (*P1F6*; 10 μg/ml) or both anti-β5 and anti-β6 (10D5; 100 μg/ml) antibodies. Note that heterologous expression of αvβ8 does not interfere with the adhesive functions, the other VN receptors present in H647 cells, αvβ5 (72) and αvβ6 (73). *Bars*, SD. *B*, β8 expression induces cell rounding on VN but not on Col I. β8-expressing cells were more rounded on VN (*a*) than the mock-infected H647 cells (*b*). There was no effect on morphology when β8-expressing or mock-infected cells were plated on Col I, an irrelevant β8 ligand (*c* and *d*). *C*, the β8-expressing cells on VN were significantly less spread than the β8 cells on Col I or the mock-infected cells on either ligand. Cells were defined as spread if lamellipodia were present and if the cell borders showed no phase enhancement ($n = 3$; *, $P < 0.01$). *Bars*, SD.

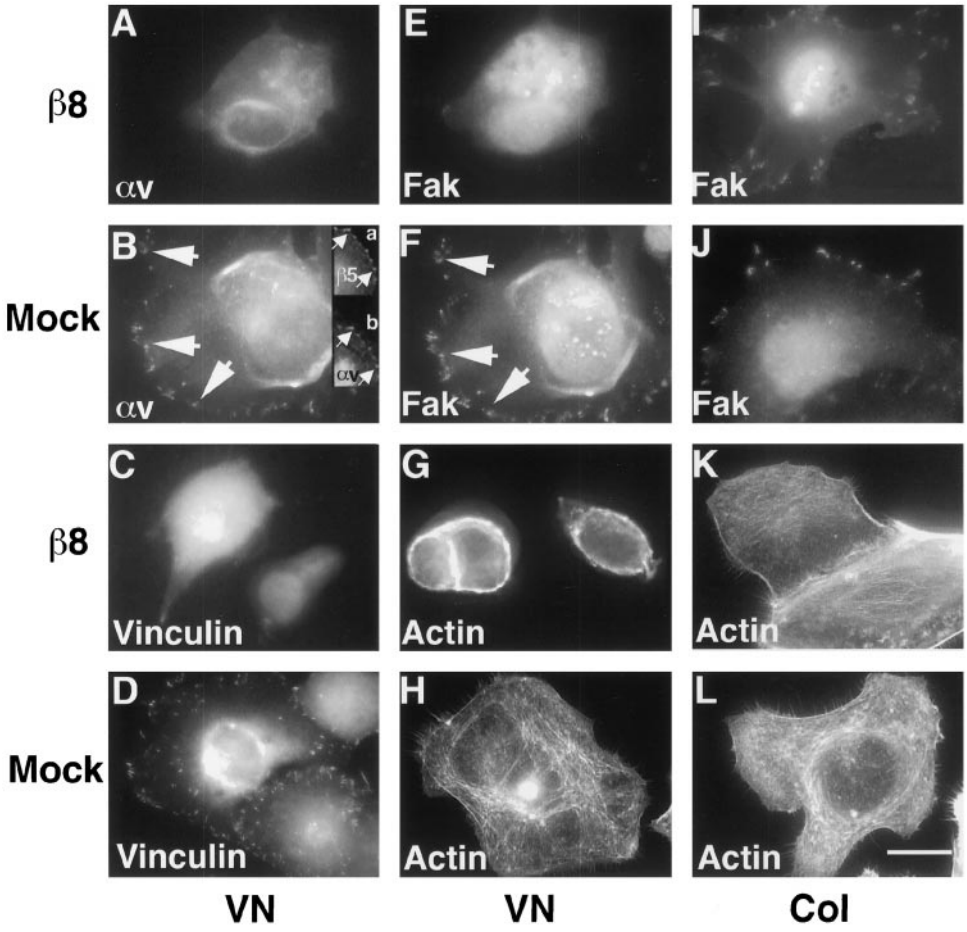

Fig. 4. Ligation of αvβ8 inhibits the focal contact localization of αvβ5 and FAK in H647 cells. The β8-expressing H647 cells, when plated on VN, displayed almost no localization of αv (*A*), vinculin (*C*), or FAK in focal contacts (*E*). In contrast, in mock-infected H647 cells plated on VN, αv (*B* and *inset b*) codistributed with β5 (*B* and *inset a*) and FAK (*F*). On VN, the mock-infected cells formed vinculin-containing focal contacts (*D*), had rope-like actin fibers at the cell periphery in addition to fully developed actin stress fibers (*H*), whereas the β8-expressing lung carcinoma cells formed rope-like actin fibers at the cell periphery and had few recognizable internal stress fibers (*G*). No differences in focal contact formation, as determined by FAK (*I* and *J*) or vinculin localization (not shown), were seen between mock-infected and β8-expressing H647 cells plated on Col I (*K* and *L*). Note that the nuclear staining seen with the αv, FAK, and vinculin antibodies is most likely nonspecific and was seen equally in both mock and β8-expressing cells. Shown is a representative experiment ($n = 4$). *Bar*, 25 μm.

blocking antibodies to the other VN receptors present in H647 cells, αvβ5 and αvβ6, no differences in adhesion to VN were seen between the β8-expressing and nonexpressing cells, indicating that adhesion to VN could not be attributed to αvβ8 (Fig. 3*A*). This is consistent with our previous findings that αvβ8-VN interactions do not mediate stable cell adhesion to VN, likely because of the divergent cytoplasmic domain of β8 (24).

Ligation of the αvβ8 Integrin Inhibits H647 Adenosquamous Lung Cancer Cell Spreading, Focal Contact Formation, and Actin Cytoskeleton Polymerization. β8-expressing cells, when plated on VN, spread less well than mock-infected cells (Fig. 3, *Ba* and *Bb*, *C*). On Col I, an irrelevant β8-ligand, β8-expressing, and mock-infected H647 cells spread similarly (Fig. 3, *Bc* and *Bd*, *C*) over a wide range of Col I coating concentrations (0.5–10 μg/ml; data not shown). Thus, the αvβ8 inhibition of cell spreading was specific to VN.

In H647 cells plated on VN, β8 expression markedly reduced the number of αv-, FAK- and vinculin-containing focal contacts in comparison with mock-infected cells (Fig. 4, *A–F*). Because in the mock-infected cells, the αv in focal contacts colocalized with β5 and FAK (Fig. 4*B*, *inset a* and *b*, and *F*), we conclude that αvβ8 ligation inhibits αvβ5 and FAK focal contact formation. As expected, αvβ8 itself does not localize to focal contacts in H647 cells, because at 4, 8, and 24 h after plating, no focal contact localization and only diffuse cytoplasmic labeling was seen using both polyclonal (cyto-1) and monoclonal (SN1) β8 antibodies (not shown). Consistent with the αvβ8 inhibition of cell spreading and inhibition of focal contact formation, β8-expressing cells, when plated on VN, displayed marked reductions in the number of recognizable actin stress fibers compared with the mock-infected cells (Fig. 4, *G* and *H*). The inhibitory effects of αvβ8 on focal contact formation and actin stress fiber formation were ligation dependent; no differences in focal contact localization or actin stress fiber formation, as determined by FAK localization or phalloidin staining, were seen between β8-expressing and mock-infected H647 cells plated on an irrelevant αvβ8 ligand, Col I (Fig. 4, *I, J* or *K, L*).

Ligation of the αvβ8 Integrin Inhibits H647 Adenosquamous Lung Cancer Cell Proliferation Independently of Apoptosis. When compared with mock-infected cells, β8-expressing H647 cells plated on VN had a lower rate of proliferation, as determined by a reduction in cell number (Fig. 5*A*) and DNA synthesis (Fig. 5*B*). These differences were not observed when cells were grown on the irrelevant β8 ligand, Col I. The inhibitory effect of β8 expression on cell growth was not attributable to apoptosis, as determined by Annexin V staining, between β8-expressing and mock-infected cells (Fig. 5*C*). Because the H647 cells could not be synchronized by serum starvation, we analyzed cell cycle distribution of nonsynchronized β8-expressing and mock-infected H647 cells plated on VN or Col I. β8-expressing cells plated on VN had a lower percentage of cells in the S phase of the cell cycle (21 ± 4%) than did β8-expressing cells on Col I (30 ± 6%) or mock-infected cells plated on either substrate (VN, 34 ± 4%; Col I, 32± 7%; $n = 17$; $P < 0.05$). Confirming our Annexin V data, DNA histograms did not reveal an apoptotic subdiploid population in β8-expressing cells plated on VN (data not shown).

Because cell spreading on two-dimensional substrates has been implicated in cell cycle control (43), we assessed the ability of β8 to influence cell growth in soft agar (nonadherent conditions, where cells were not spread). Out data show that in soft agar, expression of β8 inhibited cell growth to a similar extent as seen on a two-dimensional substrate (Fig. 5*D*).

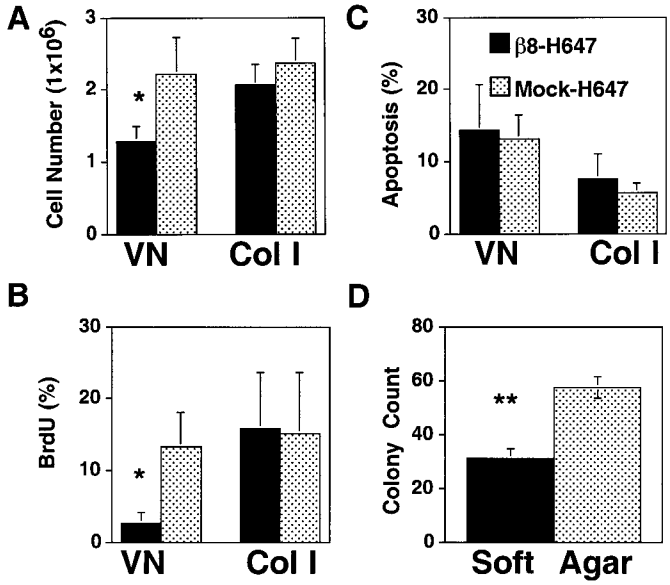

Fig. 5. Ligation of αvβ8 in H647 cells inhibits cell proliferation independently of apoptosis. *A*, nonsynchronized β8-expressing cells grown on VN for 72 h showed a significant reduction in cell number when compared with the mock-infected cells plated on VN or mock or β8-infected cells plated on Col I ($n = 4$; *, $P < 0.01$). *B*, nonsynchronized H647 lung carcinoma cells expressing β8, when grown on VN for 24 h, exhibited a significant decrease in BrdUrd incorporation when compared with the mock-infected cells plated on VN ($n = 6$) or mock- or β8-infected cells plated on Col I ($n = 3$; *, $P < 0.05$). *C*, no significant differences in percentage of apoptotic cells were seen between β8-expressing and mock-infected H647 cells grown on VN or Col I for 24 h. Shown is pooled data ($n = 3$) representing the percentage of Annexin V-positive/propidium iodide-negative, β8-expressing, and mock-infected H647 cells. *D*, β8 expression in H647 cells inhibited cell growth in soft agar with β8 expression inhibiting colony-forming ability 53% compared with the mock-infected cells ($n = 24$; **, $P < 0.0001$). *Bars: A–C*, SD; *D*, SE.

αvβ8 Expression Inhibits H647 Adenosquamous Lung Cancer Tumor Growth in Nude Mice. To assess whether the growth-inhibitory effect of β8 on H647 lung carcinoma cell growth was also manifested *in vivo*, we injected parental, mock-infected, or β8-expressing H647 cells s.c. into athymic nude mice. Parental or mock-infected H647 cells formed tumors at every injection site with satellite tumors forming at approximately half the injection sites (1.42 ± 0.50 tumors/injection site). In contrast, the β8-expressing H647 cells formed significantly fewer tumors with essentially no satellite tumors (0.91 ± 0.49 tumors/injection site; $P = 0.0047$). The tumors from mock-infected H647 cells were significantly larger than the tumors from the β8-expressing H647 cells (Fig. 6; $P < 0.0001$). Both the β8-expressing and mock-infected H647 cell tumors maintained squamous and glandular-like differentiation, consistent with the pathological description of the original lesion as adenosquamous carcinoma (Ref. 26; data not shown). Immunohistochemical analysis revealed β8 staining in the tumors formed from β8-expressing but not the mock-infected cells (data not shown).

Ligation of αvβ8 Inhibits SW480 Colon Carcinoma Cell Spreading, Focal Contact Formation, and Proliferation. To confirm that the growth-inhibitory effect of β8 was not confined to H647 cells and cell lines of pulmonary origin, we studied the effect of β8 in SW480 colon carcinoma cells, a cell line that has been well characterized for its ability to proliferate in response to heterologous expression of integrin subunits (1, 38). In SW480 cells, after retroviral transduction, we detected the αvβ8 heterodimer by FACS (Fig. 7*A*) and immunoprecipitation (not shown) and the β8 subunit by Western blotting (not shown). Consistent with previous reports, SW480 cells expressed only one αv integrin, αvβ5 (1); heterologous expression of β8 had minimal effects on surface expression of αvβ5 (Fig. 7*A*). However, β8-expression markedly decreased the formation of focal contacts (Fig. 7*A*), cell spreading (Fig. 7*B*), and cell proliferation on VN (Fig. 7*C*). Similar to our finding in H647 cells, no effects of β8 expression on stable cell adhesion to VN or Col I were seen over a coating concentration range of 1–10 μg/ml (not shown). The decreases in focal contact localization, spreading, and growth were specific for a VN substrate; no significant differences were seen between β8-expressing cells and mock-infected SW480 cells on Col I (Fig. 7). The growth-inhibitory effects of β8 were not attributable to apoptosis because the percentage of Annexin V-positive cells was not significantly different between mock-infected cells and β8-expressing SW480 cells when grown on either VN or Col I (in a representative experiment on VN: β8 4% and Mock 7%; and on Col I: β8 3% and Mock 10%). Finally, when grown in soft agar, SW480 β8-expressing cells formed 69% fewer colonies (>100 mM) than did mock-infected cells (3.1± 2.3 *versus* 10.0± 5.2/well; $P < 0.01$).

The β8 Cytoplasmic Domain Functions as an Inhibitor of Cell Spreading, Focal Contact Formation, and Proliferation. To identify a role for the β8 cytoplasmic domain in growth inhibition, we used a chimeric subunit composed of the β6 extracellular and transmembrane domains coupled to the β8 cytoplasmic domain (β6/8). This subunit was efficiently expressed in SW480 colon carcinoma cells, and when β6- and β6/8-expressing pools were sorted, similar levels of surface expression of β6 and β6/8 were achieved (Fig. 8*A*). Expression of the β6/8 chimera significantly inhibited αv and FAK focal contact localization (Fig. 8*A*), inhibited cell spreading (Fig. 8*B*), and inhibited growth (Fig. 8*C*) relative to the β6- and mock-infected controls. The differences in cell growth were not attributable to apoptosis; no significant differences were seen in the percentage of apoptotic cells between β6/8- and β6-expressing cells grown on FN (in a representative experiment: β6/8 4.5% and β6 6.4%). These inhibitory effects were specific for the β6 ligand fibronectin because no significant differences in focal contact localization, spreading, or growth were seen among β6-, β6/8- and mock-infected cells on an irrelevant β6 ligand, Col I (not shown). Finally, these findings show that the effects of β8 are unlikely to be attributable to an artifact of introduction of a foreign β-integrin subunit, because introduction of the full-

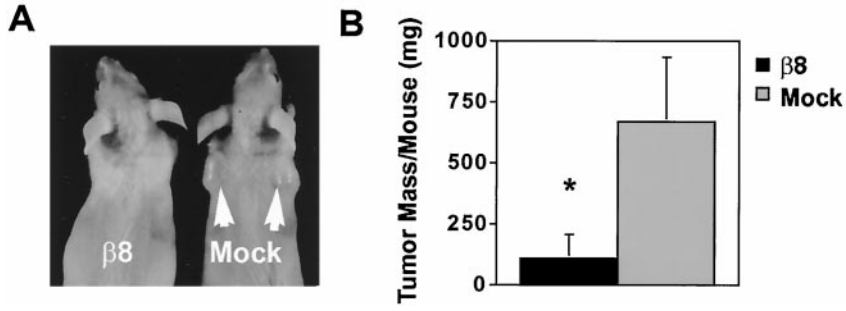

Fig. 6. β8 expression in H647 cells inhibits tumor growth in nude mice. *A*, large tumors formed in the mice inoculated with mock-infected H647 cells (*arrows*) but not in the mice inoculated with β8-expressing cells (on *left*). *B*, the β8-expressing H647 cells produced a mean tumor weight/mouse (0.11± 0.10 g/tumor) 84% less than did the mock-infected H647 cells (0.67± 0.26 g/tumor; *, $P < 0.001$). The data represent three separate experiments with six mice in each group (total tumors analyzed: β8, $n = 66$; Mock, $n = 102$). *Bars*, SD.

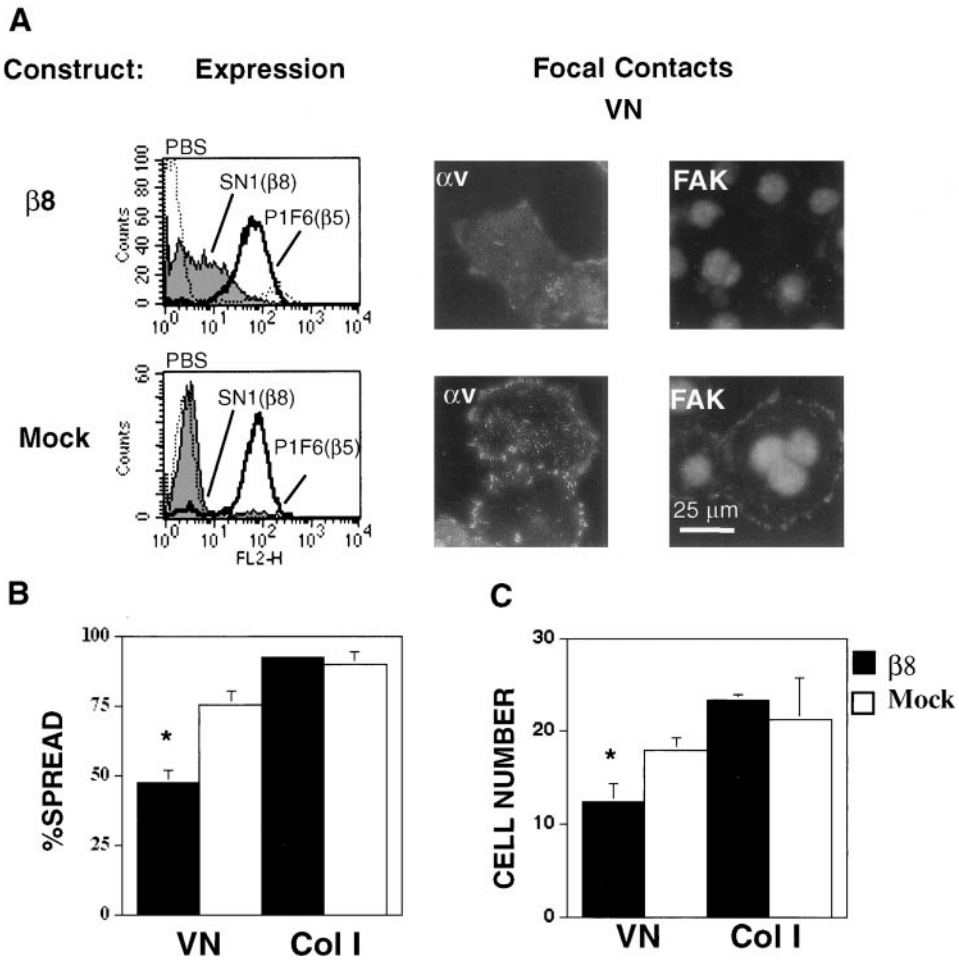

Fig. 7. Ligation of αvβ8 inhibits cell spreading, focal contact formation, and cell proliferation in SW480 colonic carcinoma cells. SW480 cells were transduced with β8, sorted for the highest expressing cells and used for focal contact localization, cell spreading, and cell proliferation assays. *A: Expression*, histograms of cells stained with anti-αv (L230), anti-β5 (P1F6) or no primary (PBS); *Focal Contacts:* on VN as determined by anti-αv (L230) and anti-FAK. Because SW480 only express one VN receptor, αvβ5 (33), αv focal contact localization is an estimate of αvβ5. β8 staining was diffuse and was not found in focal contacts as determined by staining with the anti-β8 monoclonal antibody SN1. Shown is a representative experiment ($n = 3$). *B: % Spread*, spread test cells/all cells on VN (*bars*, SE; $n = 3$; $P < 0.01$). *C: Growth*, cell number ($\times 10^4$) after 72 h on VN (*bars*, SE; $n = 20$; $*$, $P < 0.001$).

length β6 subunit into SW480 cells had no effect on cell growth (Fig. 8*C*).

Surprisingly, expression of β6 slightly decreased the surface expression of αvβ5 relative to that seen in β6/8 and mock-infected cells (Fig. 8*A*). However, when compared with the mock-infected control cells, this slight decrease did not impact focal contact localization (Fig. 8*A*), cell spreading (Fig. 8*B*), or cell proliferation (Fig. 8*C*) compared with the mock-infected cells.

Ligation of αvβ8 Increases $p21^{Cip1}$ Expression, a Possible Mechanism of Growth Inhibition. Ligation of αvβ8 in SW480 and H647 cells resulted in increased $p21^{Cip1}$ expression compared with mock-infected cells. Thus, in both cell lines, the $p21^{Cip1}$ expression was higher when β8-expressing cells were plated on VN as compared with Col I (Fig. 9).

DISCUSSION

The present study demonstrates that αvβ8 is a growth-inhibitory molecule and provides the first evidence for an *in vivo* function of the divergent integrin subunit β8. This conclusion is based on our data showing that: (*a*) αvβ8 is expressed in normal airway epithelium and its expression is generally absent in tumors derived from airway epithelium; (*b*) αvβ8 mediates cell shape changes and inhibits focal contact and actin cytoskeleton formation; (*c*) αvβ8 inhibits cell proliferation without inducing apoptosis; (*d*) αvβ8 inhibits cell growth in association with induction of $p21^{Cip1}$; and (*e*) αvβ8 can inhibit tumor growth in nude mice. Taken together, these findings implicate the integrin αvβ8 as a negative growth regulatory molecule of human airway epithelium and provide the first evidence that αv integrins, generally regarded as promoters of tumor growth (2, 4), may also be inhibitors of tumor growth.

In human airway epithelium, the role of integrin-ECM interactions in the negative regulation of cell growth has not been reported. This is in contrast to other epithelial types, such as breast, colon, and prostate, where integrin-ECM interactions have been have been implicated in the maintenance of epithelial homeostasis (44–47). For instance, in breast or colonic epithelial cell lines, alterations in the expression levels of β1 integrins are sufficient to alter cellular proliferation and differentiation (44, 47). In addition, the expression of individual integrin β-subunits with sequence divergence in their cytoplasmic domains (*i.e.*, the alternative splice variants of the integrin β1 subunit and the β4 integrin subunit) has been shown to mediate growth inhibition (19, 20, 48). Until this report, there has been no evidence implicating integrins, divergent or otherwise, in mediating growth inhibition in the human airway epithelium. As such, our data provide novel insights into the mechanisms of airway epithelial cell growth regulation.

To investigate the mechanism of αvβ8-mediated growth inhibition, we initially determined the impact of αvβ8 ligation on the formation of focal adhesions, which represent integrin signaling complexes at points of cell-ECM contact (49). We found that αvβ8-VN interactions inhibited the focal contact localization of the other endogenous αv-heterodimers present in H647 and SW480 cells. Furthermore, αvβ8-VN interactions inhibited cell spreading without affecting the stable cell adhesion of these endogenous αv heterodimers. Because αvβ8 did not affect stable cell

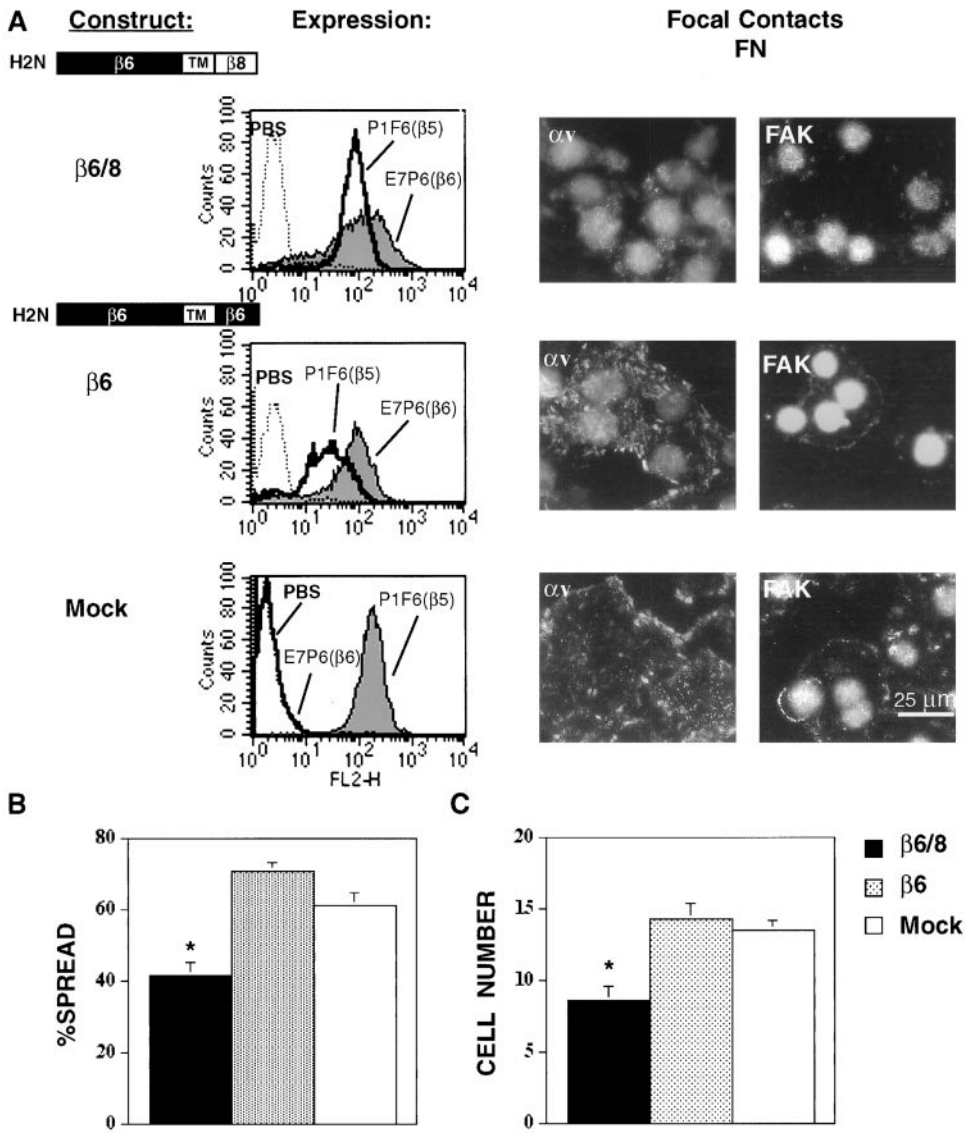

Fig. 8. Inhibition of focal contact formation, cell spreading, and cell proliferation is mediated by the β8 cytoplasmic domain. SW480 cells were transduced with the β6 and β6/8 chimeras and sorted for equal levels of surface expression of the β6 extracellular domain. Mock-infected cells were sorted in parallel. *A: Expression*, histograms of cells stained with anti-β6 (E7P6) or anti-β5 (P1F6). Shown is a representative experiment ($n = 4$). Note that a slight decrease in the surface levels of αvβ5 was seen in the β6-infected cells relative to the β6/8- and mock-infected cells. This slight decrease did not significantly impact the ability of the β6 transfectants to interact with the αvβ6 ligand, FN. *Focal Contacts*, as determined by anti-αv and anti-FAK staining on fixed and permeabilized β6-, β6/8- and mock-infected SW480 cells plated on the αvβ6 ligand, FN. Shown is a representative experiment ($n = 3$). *B: %Spread*, the percentage of spread test cells/percentage of all cells on FN (*bars*, SE; $n = 3$; $P < 0.05$). *C*, for growth, cell number ($\times 10^4$) after 72 h on FN compared with mock-infected control (*bars*, SE; $n = 6$; $*$, $P < 0.01$).

adhesion to VN, we concluded that the αvβ8 inhibition of cell spreading, focal contact formation, and cell proliferation were likely not attributable to competition for ligand binding sites on VN. It appeared more likely that the inhibitory effects were mediated by the cytoplasmic domain of β8. To test the role of the β8 cytoplasmic domain in mediating cell shape changes and growth inhibition, we used a chimeric receptor consisting of the β6 extracellular domain coupled to the β8 cytoplasmic domain. We chose this chimera because β6 has been shown to promote the growth of SW480 cells and because β6 truncation mutants have been successfully generated in SW480 cells without inhibiting the cell adhesion and spreading functions of the endogenous fibronectin receptors, αvβ5 or a5β1 (1, 50). Using the β6/8 chimera, in SW480 cells we demonstrated significant inhibition of focal contact localization, spreading, and growth on the αvβ6 ligand, fibronectin. Our conclusion from this experiment is that the β8 cytoplasmic domain is sufficient to induce all of the β8 inhibitory effects on cell shape, focal contact localization, and cell growth that we observed in SW480 cells with the full-length β8 subunit.

One possible mechanism for the β8-induced growth inhibition is through the β8 cytoplasmic domain-mediated interference of FAK function. Upon integrin ligation, FAK, a cytoplasmic tyrosine kinase, has been shown to associate with the tyrosine kinase Src and triggers activation of components of the mitogen-activated protein kinase pathway (51, 52). Furthermore, inhibition of FAK localization to focal contacts (independent of its phosphorylation state) has been linked to up-regulation of $p21^{Cip1}$ and inhibition of cell growth (53). Therefore, αvβ8-meditated inhibition of localization of FAK from focal contacts could uncouple integrin signaling from the mitogen-activated protein kinase pathway, ultimately leading to the downstream induction of $p21^{Cip1}$, an effector directly involved in the inhibition of cell cycle progression (54). Furthermore, because SW480 cells have loss of functional p53 (55) and transforming growth factor-β responsiveness (56), two major pathways of $p21^{Cip1}$ regulation (57), the pathway by which αvβ8-VN interactions can induce $p21^{Cip1}$ expression in SW480 cells, is apparently transforming growth factor-β and p53 independent.

The mechanism by which αvβ8 mediates inhibition of localization of FAK to focal contacts likely involves the β8 cytoplasmic domain because the β6/8 chimera can inhibit focal contact localization of FAK. Because we observed that β8 itself is not found in focal contacts, an expected result considering that the β8 cytoplasmic domain lacks all known focal contact localization motifs (13, 23), it is unlikely that the β8 cytoplasmic domain directly displaces FAK from focal contacts. More likely, the β8 cytoplasmic domain inhibits FAK localization indirectly. Interestingly, the β1B splice variant of the β1 integrin subunit has also been shown to inhibit FAK localization

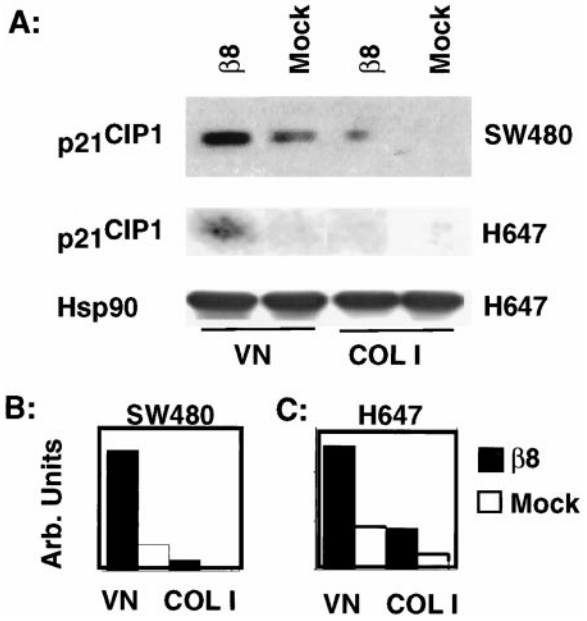

Fig. 9. αvβ8 ligation is associated with increased expression of $p21^{Cip1}$. *A*, SW480 or H647 cells either β8- or mock-infected were plated on either VN or Col I. After 24 h, the cells were lysed, and 40 μg of total protein were analyzed for $p21^{Cip1}$ expression by Western blotting. Shown is a representative experiment ($n = 3$) demonstrating that $p21^{Cip1}$ expression is increased in β8-expressing SW480 and H647 cells plated on VN relative to Col I. Equal protein loading was confirmed by immunoblotting with an antibody against heat shock protein 90α subunit. *B*, densitometric analysis of Western blot (NIH Image) in arbitrary units.

without itself localizing to focal contacts (58, 59), suggesting that β8 and β1B could inhibit FAK function through similar pathways.

Another possible mechanism for β8 inhibition of FAK localization and inhibition of cell growth is through the generation of specific inhibitory signals initiated through the β8 cytoplasmic domain, resulting in the downstream up-regulation of $p21^{Cip1}$. Consistent with this, the β1C alternative splice variant of β1 has been shown to induce the cyclin-dependent kinase inhibitor $p27^{kip1}$ and thereby inhibit cell growth (46). Interestingly, unlike β8 and β1B, forced expression of β1C does not alter focal contact formation and, thus, is likely acting in a FAK-independent pathway (19). Therefore, it appears that divergent integrins or alternative splice variants can inhibit cell growth through distinct FAK-dependent or FAK-independent mechanisms.

Because of the well-known observations in fibroblasts that link changes in cell shape with inhibition of cell growth (43, 60–63), we considered whether αvβ8-mediated cell shape changes might themselves be responsible for cell growth inhibition. Cells in culture require anchorage, spreading, and an organized cytoskeleton to progress through S phase; when deprived of anchorage or cell spreading, the cell cycle machinery is inhibited concurrent with up-regulation of cyclin-dependent kinase inhibitors (60, 64, 65). Because β8 inhibited growth in soft agar under conditions where cells are not obviously spread, it is possible that β8-mediated growth inhibition and inhibition of cell spreading are independent functions. However, growth in soft agar is not truly a test of cell shape-independent growth (cells in soft agar can assemble their own pericellular matrix, which may allow cell shape changes), and thus, more definitive evidence separating β8-mediated cell shape changes and growth inhibition await further experimentation.

Ultimately, for a clearer understanding of the biological significance of integrin-ECM interactions, a three-dimensional cellular microenvironment is crucial (44, 45, 66). Thus, we tested the ability of β8 to inhibit lung cancer cell growth in nude mice. Our findings demonstrate that β8 can dramatically inhibit H647 tumor growth *in vivo*. The *in vivo* milieu is complex and rich in diverse cell types secreting growth factors and multiple ECM ligands (67), and the H647 adenosquamous cells express receptors for many of these receptors and ECM ligands. Thus, *in vivo*, it appears that αvβ8 is capable of generating growth-inhibitory signals that can override the integrated inputs from a complex repertoire of growth-promoting signals.

What is the function of αvβ8 ligation in normal airway epithelium? It is possible that β8 might normally function in airway epithelium to maintain a quiescent state. Consistent with this, β8 is predominately expressed in basal cells, a cell type that normally has a very low rate of proliferation (6). Because VN is expressed in the lung (68–70), αvβ8-VN interactions might function normally to maintain epithelial quiescence or to maintain the characteristic rounded shape of basal cells. Several other VN receptors have been reported to be expressed in basal cells of airway epithelium including the integrins αvβ3 (7), αvβ5, and αvβ6 (10). Because αvβ3, αvβ5, and αvβ6 have been implicated in growth promotion (1, 2, 4), it is possible that αvβ8 might function to counterbalance the growth-promoting signals generated by these integrins. Thus, αvβ8 may be crucial to the homeostatic complement of integrins in human airway epithelium (10, 71).

In summary, our findings demonstrate that the β8 integrin subunit is growth inhibitory in epithelial cells and that the divergent β8 cytoplasmic domain is sufficient to confer growth inhibition. The mechanism of αvβ8-mediated growth inhibition is likely to involve inhibition of focal contact formation, FAK localization, and induction of the cyclin-dependent kinase inhibitor, $p21^{Cip1}$. These data support an emerging paradigm that one important function of divergent or alternatively spliced integrin β-cytoplasmic domains is to inhibit cell growth (21, 22, 48).

ACKNOWLEDGMENTS

We thank Jody Baron, Amha Atakilit, Naftali Kaminski, Nancy Boudreau, Dean Sheppard, and Robert Pytela for helpful comments and reagents.

REFERENCES

1. Agrez, M., Chen, A., Cone, R. I., Pytela, R., and Sheppard, D. The αvβ6 integrin promotes proliferation of colon carcinoma cells through a unique region of the β6 cytoplasmic domain. J. Cell Biol., *127:* 547–556, 1994.
2. Albelda, S. M., Mette, S. A., Elder, D. E., Stewart, R., Damjanovich, L., Herlyn, M., and Buck, C. A. Integrin distribution in malignant melanoma: association of the β3 subunit with tumor progression. Cancer Res., *50:* 6757–6764, 1990.
3. Brooks, P. C., Strömblad, S., Klemke, R., Visscher, D., Sarkar, F. H., and Cheresh, D. A. Antiintegrin αvβ3 blocks human breast cancer growth and angiogenesis in human skin. J. Clin. Investig., *96:* 1815–1822, 1995.
4. Felding-Habermann, B., Mueller, B. M., Romerdahl, C. A., and Cheresh, D. A. Involvement of integrin αv gene expression in human melanoma tumorigenicity. J. Clin. Investig., *89:* 2018–2022, 1992.
5. Varner, J. A., Brooks, P. C., and Cheresh, D. A. The integrin αvβ3: angiogenesis and apoptosis. Cell Adhes. Commun., *3:* 367–374, 1995.
6. Boers, J. E., Ambergen, A. W., and Thunnissen, F. B. J. M. Number and proliferation of basal and parabasal cells in normal human airway epithelium. Am. J. Resp. Crit. Care Med., *157:* 2000–2006, 1998.
7. Hicks, W., Jr., Hall, L., III, Sigurdson, L., Stewart, C., Hard, R., Winston, J., and Lwebuga-Mukasa, J. Isolation and characterization of basal cells from human upper respiratory epithelium. Exp. Cell Res., *237:* 357–363, 1997.
8. Mette, S. A., Pilewski, J., Buck, C. A., and Albelda, S. M. Distribution of integrin cell adhesion receptors on normal bronchial epithelial cells and lung cancer cells *in vitro* and *in vivo*. Am. J. Resp. Cell. Mol. Biol., *8:* 562–572, 1993.
9. Pilewski, J. M., Latoche, J. D., Arcasoy, S. M., and Albelda, S. M. Expression of integrin cell adhesion receptors during human airway epithelial repair *in vivo*. Am. J. Physiol, *273:* L256–L263, 1997.
10. Wang, A., Yokosaki, Y., Ferrando, R., Balmes, J., and Sheppard, D. Differential regulation of airway epithelial integrins by growth factors. Am. J. Resp. Cell. Mol. Biol., *15:* 664–672, 1996.
11. Pisani, P., Parkin, D. M., Bray, F., and Ferlay, J. Estimates of the worldwide mortality from 25 cancers in 1990. Int. J. Cancer, *83:* 18–29, 1999.
12. Murray, C. J., and Lopez, A. D. Mortality by cause for eight regions of the world: Global Burden of Disease Study. Lancet, *349:* 1269–1276, 1997.
13. Reszka, A. A., Hayashi, Y., and Horwitz, A. F. Identification of amino acid sequences in the integrin β1, cytoplasmic domain implicated in cytoskeletal association. J. Cell Biol., *117:* 1321–1330, 1992.
14. Filardo, E. J., Brooks, P. C., Deming, S. L., Damsky, C., and Cheresh, D. A. Requirement for the NPXY motif in the integrin β3 cytoplasmic tail for melanoma cell migration *in vivo* and *in vitro*. J. Cell Biol., *130:* 441–450, 1995.

15. Dixit, R. B., Chen, A., Chen, J., and Sheppard, D. Identification of a sequence within the integrin β6 subunit cytoplasmic domain that is required to support the specific effect of αvβ6 on proliferation in three-dimensional culture. J. Biol. Chem., *271:* 25976–25980, 1996.
16. LaFlamme, S. E., Homan, S. M., Bodeau, A. L., and Mastangelo, A. M. Integrin cytoplasmic domains as connectors to the cell's signal transduction apparatus. Matrix Biol., *16:* 153–163, 1997.
17. O'Toole, T. E., Katagiri, Y., Faull, R. J., Peter, K., Tamura, R., Quaranta, V., Loftus, J. C., Shattil, S. J., and Ginsberg, M. H. Integrin cytoplasmic domains mediate inside-out signal transduction. J. Cell Biol., *124:* 1047–1059, 1994.
18. Schaller, M. D., Hilderbrand, J. D., Sannon, J. D., Fox, J. W., Vines, R. R., and Parsons, J. T. Focal adhesion kinase and paxillin bind to peptides mimicking β integrin cytoplasmic domains. J. Cell Biol., *130:* 1181–1187, 1994.
19. Meredith, J., Jr., Takada, Y., Fornaro, M., Languino, L. R., and Schwartz, M. A. Inhibition of cell cycle progression by the alternatively spliced integrin $\beta 1_c$. Science (Washington DC), *269:* 1569–1572, 1995.
20. Belkin, A. M., and Retta, S. F. β1D integrin inhibits cell cycle progression in normal myoblasts and fibroblasts. J. Biol. Chem., *273:* 15234–15240, 1998.
21. Fornaro, M., Zheng, D-Q., and Languino, L. R. The novel structural motif Gln^{795}-Gln^{802} in the integrin $\beta 1_C$ cytoplasmic domain regulates cell proliferation. J. Biol. Chem., *270:* 24666–24669, 1995.
22. Fornaro, M., and Languino, L. R. Alternatively spliced variants: a new view of the integrin cytoplasmic domains. Curr. Opin. Cell Biol., *16:* 185–193, 1997.
23. Moyle, M., Napier, M. A., and McLean, J. W. Cloning and expression of a divergent integrin subunit β8. J. Biol. Chem., *266:* 19650–19658, 1991.
24. Nishimura, S. L., Sheppard, D., and Pytela, R. Integrin αvβ8: interaction with vitronectin and functional divergence of the β8 cytoplasmic domain. J. Biol. Chem., *269:* 28708–28715, 1994.
25. Nishimura, S. L., Boylen, K. P., Einheber, S., Milner, T. A., Ramos, D. M., and Pytela, R. Synaptic and glial localization of the integrin αvβ8 in mouse and rat brain. Brain Res., *791:* 271–282, 1998.
26. Mitsudomi, T., Viallet, J., Mulshine, J. L., Linnoila, R. I., Minna, J. D., and Gazdar, A. F. Mutations of *ras* genes distinguish a subset of non-small-cell lung cancer cell lines from small-cell lung cancer cell lines. Oncogene, *6:* 1353–1362, 1991.
27. Mitsudomi, T., Steinberg, S. M., Nau, M. M., Carbone, D., D'Amico, D., Bodner, S., Oie, H. K., Linnoila, R. I., Mulshine, J. L., Minna, J. D., and Gazdar, A. F. *p53* gene mutations in non-small-cell lung cancer cell lines and their correlation with the presence of ras mutations and clinical features. Oncogene, *7:* 171–180, 1992.
28. Tsai, C. M., Chang, K. T., Perng, R. P., Mitsudomi, T., Chen, M. H., Kadoyama, C., and Gazdar, A. F. Correlation of intrinsic chemoresistance of non-small-cell lung cancer cell lines with HER-2/*neu* gene expression but not with *ras* gene mutations. J. Natl. Cancer Inst., *85:* 897–901, 1993.
29. Cozens, A. L., Yezzi, M. J., Chin, L., Simon, E. M., Finkbeiner, W. E., Wagner, J. A., and Gruenert, D. C. Characterization of immortal cystic fibrosis tracheobronchial gland epithelial cells [published erratum appears in Proc. Natl. Acad. Sci. USA, *89:* 7849, 1992]. Proc. Natl. Acad. Sci. USA, *89:* 5171–5175, 1992.
30. Cozens, A. L., Yezzi, M. J., Kunzelmann, K., Ohrui, T., Chin, L., Eng, K., Finkbeiner, W. E., Widdicombe, J. H., and Gruenert, D. C. CFTR expression and chloride secretion in polarized immortal human bronchial epithelial cells. Am. J. Resp. Cell Mol. Biol., *10:* 38–47, 1994.
31. Kinsella, T. M., and Nolan, G. Episomal vectors rapidly and stably produce high-titer recombinant retrovirus. Hum. Gene Ther., *7:* 1405–1413, 1996.
32. Newman, P. J., Allen, R. W., Kahn, R. A., and Kunicki, T. J. Quantitation of membrane glycoprotein IIIa on intact human platelets using the monoclonal antibody, AP-3. Blood, *65:* 227–232, 1985.
33. Weinacker, A., Chen, A., Agrez, M., Cone, R., Nishimura, S. L., Wayner, E., Pytela, R., and Sheppard, D. Role of the integrin αvβ6 in cell attachment to fibronectin, heterologous expression of intact and secreted forms of the receptor. J. Biol. Chem., *269:* 6940–6948, 1994.
34. Morgenstern, J. P., and Land, H. Advanced mammalian gene transfer: high titer retroviral vectors with multiple drug selection markers and a complementary helper-free packaging line. Nucl. Acids Res., *18:* 3587–3596, 1990.
35. Warrens, A. N., Jones, M. D., and Lechler, R. I. Splicing by overlap extension by PCR using asymmetric amplification: an improved technique for the generation of hybrid proteins of immunological interest. Gene (Amst.), *186:* 29–35, 1997.
36. Sheppard, D., Rozzo, C., Starr, L., Quaranta, V., Erle, D. J., and Pytela, R. Complete amino acid sequence of a novel integrin β subunit (β6) identified in epithelial cells using the polymerase chain reaction. J. Biol. Chem., *265:* 11502–11507, 1990.
37. Pytela, R., Suzuki, S., Breuss, J., Erle, D. J., and Sheppard, D. Polymerase chain reaction cloning with degenerate primers: homology-based identification of adhesion molecules. Methods Enzymol., *245:* 420–451, 1994.
38. Yokosaki, Y., Monis, H., Chen, J., and Sheppard, D. Differential effects of the integrins α9β1, αvβ3, and αvβ6 on cell proliferative responses to tenascin. Roles of the β subunit extracellular and cytoplasmic domains. J. Biol. Chem., *271:* 24144–24150, 1996.
39. Yatohgo, T., Izumi, M., Kashiwagi, H., and Hayashi, M. Novel purification of vitronectin from human plasma by heparin affinity chromatography. Cell Struct. Funct., *13:* 281–292, 1988.
40. Montesano, R., Mouron, P., Amherdt, M., and Orci, L. Collagen matrix promotes reorganization of pancreatic endocrine cell monolayers into islet-like organoids. J. Cell Biol., *97:* 935–939, 1983.
41. Shi, S. R., Key, M. E., and Kalra, K. L. Antigen retrieval in formalin-fixed, paraffin-embedded tissues: an enhancement method for immunohistochemical staining based on microwave oven heating of tissue sections. J. Histochem. Cytochem., *39:* 741–748, 1991.
42. Broaddus, V. C., Yang, L., Scavo, L. M., Ernst, J. D., and Boylan, A. M. Asbestos induces apoptosis of human and rabbit pleural mesothelial cells via reactive oxygen species. J. Clin. Investig., *98:* 2050–2059, 1996.
43. Folkman, J., and Moscona, A. Role of cell shape change in growth control. Nature (Lond.), *273:* 345–349, 1978.
44. Weaver, V. M., Petersen, O. W., Wang, F., Larabell, C. A., Briand, P., Damsky, C., and Bissell, M. J. Reversion of the malignant phenotype of human breast cells in three-dimensional culture and *in vivo* by integrin blocking antibodies. J. Cell Biol., *137:* 231–245, 1997.
45. Bissell, M. J., Weaver, V. M., Lelievre, S. A., Wang, F., Petersen, O. W., and Schmeichel, K. L. Tissue structure, nuclear organization, and gene expression in normal and malignant breast. Cancer Res., *59* (Suppl.)*:* 1757s–1764s, 1999.
46. Fornaro, M., Tallini, G., Zheng, D. Q., Flanagan, W. M., Manzotti, M., and Languino, L. R. p27(kip1) acts as a downstream effector of and is coexpressed with the $\beta 1_C$ integrin in prostatic adenocarcinoma. J. Clin. Investig., *103:* 321–329, 1999.
47. Varner, J. A., Emerson, D. A., and Juliano, R. L. Integrin α5β1 expression negatively regulates cell growth: reversal by attachment to fibronectin. Mol. Biol. Cell, *6:* 725–740, 1995.
48. Clarke, A. S., Lotz, M. M., Chao, C., and Mercurio, A. M. Activation of the p21 pathway of growth arrest and apoptosis by the b4 integrin cytoplasmic domain. J. Biol. Chem., *270:* 22673–22676, 1995.
49. Hynes, R. O. Integrins: versatility, modulation, and signaling in cell adhesion. Cell, *69:* 11–25, 1992.
50. Cone, R. I., Weinacker, A., Chen, A., and Sheppard, D. Effects of β subunit cytoplasmic domain deletions on the recruitment of the integrin αvβ6 to focal contacts. Cell Adhes. Commun., *2:* 101–113, 1994.
51. Schlaepfer, D. D., and Hunter, T. Focal adhesion kinase overexpression enhances Ras-dependent integrin signaling to ERK2/mitogen-activated protein kinase through interaction with and activation of c-src. J. Biol. Chem., *272:* 13189–13195, 1997.
52. Xing, Z., Chen, H. C., Nowlen, J. K., Taylor, S. J., Shalloway, D., and Guan, J. L. Direct interaction of v-Src with the focal adhesion kinase mediated by the Src SH2 domain. Mol. Biol. Cell, *5:* 413–421, 1994.
53. Zhao, J. H., Reiske, H., and Guan, J. L. Regulation of the cell cycle by focal adhesion kinase. J. Cell Biol., *143:* 1997–2008, 1998.
54. Harper, J. W., Adami, G. R., Wei, N., Keyomarsi, K., and Elledge, S. J. The p21 Cdk-interacting protein Cip1 is a potent inhibitor of G1 cyclin-dependent kinases. Cell, *75:* 805–816, 1993.
55. Abarzua, P., LoSardo, J. E., Gubler, M. L., and Neri, A. Microinjection of monoclonal antibody PAb421 into human SW480 colorectal carcinoma cells restores the transcription activation function to mutant p53. Cancer Res., *55:* 3490–3494, 1995.
56. Calonge, M. J., and Massagué, J. Smad4/DPC4 silencing and hyperactive Ras jointly disrupt transforming growth factor-β antiproliferative responses in colon cancer cells. J. Biol. Chem., *274:* 33637–33643, 1999.
57. Datto, M. B., Li, Y., Panus, J. F., Howe, D. J., Xiong, Y., and Wang, X. F. Transforming growth factor β induces the cyclin-dependent kinase inhibitor p21 through a p53-independent mechanism. Proc. Natl. Acad. Sci. USA, *92:* 5545–5549, 1995.
58. Retta, S. F., Balzac, F., Ferraris, P., Belkin, A. M., Fassler, R., Humphries, M. J., De Leo, G., Silengo, L., and Tarone, G. β1-integrin cytoplasmic subdomains involved in dominant negative function. Mol. Biol. Cell, *9:* 715–731, 1998.
59. Balzac, F., Retta, S. F., Albini, A., Melchiorri, A., Koteliansky, V. E., Geuna, M., Silengo, L., and Tarone, G. Expression of β1B integrin isoform in CHO cells results in a dominant negative effect on cell adhesion and motility. J. Cell Biol., *127:* 557–565, 1994.
60. Assoian, R. K. Anchorage-dependent cell cycle progression. J. Cell Biol., *136:* 1–4, 1997.
61. Bottazzi, M. E., Zhu, X., Bohmer, R. M., and Assoian, R. K. Regulation of p21(cip1) expression by growth factors and the extracellular matrix reveals a role for transient ERK activity in G1 phase. J. Cell Biol., *146:* 1255–1264, 1999.
62. Guadagno, T. M., Ohtsubo, J., Roberts, J. M., and Assoian, R. K. A link between cyclin A expression and adhesion-dependent cell cycle progression. Science (Washington DC), *262:* 1572–1575, 1993.
63. Zhu, X., Ohtsubo, M., Böhmer, R. M., Roberts, J. M., and Assoian, R. K. Adhesion-dependent cell cycle progression linked to the expression of cyclin D1, activation of cyclin E-cdk2, and phosphorylation of the retinoblastoma protein. J. Cell Biol., *133:* 391–403, 1996.
64. Huang, S., Chen, C. S., and Ingber, D. E. Control of cyclin D1, p27(Kip1), and cell cycle progression in human capillary endothelial cells by cell shape and cytoskeletal tension. Mol. Biol. Cell, *9:* 3179–3193, 1998.
65. Fang, F., Orend, G., Watanabe, N., Hunter, T., and Ruoslahti, E. Dependence of cyclin E-cdk2 kinase activity on cell anchorage. Science (Washington DC), *271:* 499–502, 1996.
66. Schmeichel, K. L., Weaver, V. M., and Bissell, M. J. Structural cues from the tissue microenvironment are essential determinants of the human mammary epithelial cell phenotype. J. Mamm. Gland Biol. Neopl., *3:* 201–213, 1998.
67. Boudreau, N., and Bissell, M. J. Extracellular matrix signaling: integration of form and function in normal and malignant cells. Curr. Opin. Cell. Biol., *10:* 640–646, 1998.
68. Pohl, W. R., Conlan, M. G., Thompson, A. B., Ertl, R. F., Romberger, D. J., Mosher, D. F., and Rennard, S. I. Vitronectin in bronchoalveolar lavage fluid is increased in patients with interstitial lung disease. Am. Rev. Respir. Dis., *143:* 1369–1375, 1991.
69. Teschler, H., Pohl, W. R., Thompson, A. B., Konietzko, N., Mosher, D. F., Costabel, U., and Rennard, S. I. Elevated levels of bronchoalveolar lavage vitronectin in hypersensitivity pneumonitis. Am. Rev. Respir. Dis., *147:* 332–337, 1993.
70. Sieffert, D., Iruela-Arispe, M. L., Sage, E. H., and Loskutoff, D. J. Distribution of vitronectin mRNA during murine development. Dev. Dynam., *203:* 71–79, 1995.
71. Sheppard, D. Airway epithelial integrins: why so many? Am. J. Resp. Cell Mol. Biol., *19:* 349–351, 1998.
72. Smith, J. W., Vestal, D. J., Irwin, S. V., Burke, T. A., and Cheresh, D. A. Purification and functional characterization of integrin αvβ5. An adhesion receptor for vitronectin. J. Biol. Chem., *265:* 11008–11013, 1990.
73. Huang, X., Wu, J., Farese, R., Jr., and Sheppard, D. The integrin αvβ6 is critical for keratinocyte migration on both its known ligand, fibronectin, and on vitronectin. J. Cell Sci., *111:* 2189–2196, 1997.